IEEE Access
Multidisciplinary | Rapid Review | Open Access Journal

Received December 29, 2019, accepted January 7, 2020, date of publication January 14, 2020, date of current version February 4, 2020.

Digital Object Identifier 10.1109/ACCESS.2020.2966626

Design of Wideband Beamforming Metasurface With Alternate Absorption

SAEED UR RAHMAN[1], QUNSHENG CAO[1], IGNACIO GIL[2], MUHAMMAD SAJJAD[1], AND YI WANG[1], (Member, IEEE)

[1]College of Electronic and Information Engineering, Nanjing University of Aeronautics and Astronautics (NUAA), Nanjing 210016, China
[2]Department of Electronic Engineering, Universitat Politècnica de Catalunya, 08222 Terrassa, Spain

Corresponding author: Qunsheng Cao (qunsheng@nuaa.edu.cn)

This work was supported by the National Natural Science Foundation of China under Grant number 61871219 and Ministry of Science, Technology and Information (MOSTI), Malaysia, under Science Fund project number: 03-02-02-SF0216.

ABSTRACT In this paper, we propose a periodic structure that is capable of alternating between absorption and radiation mode. The designed periodic structure consists of an array of 6×6 square shaped unit cell. Each unit cell consists of a multi-layered structure, with dimensions of 0.5λ×0.5λ. The resonators are placed on the top layer and the feeding network is designed and implemented on the bottom layer. The ground layer is sandwiched between the two dielectric substrates. All resonators are connected to a 50Ω feed-line using the corporate feeding technique. To achieve broadband absorption, lumped resistors are inserted into the resonators. The proposed metasurface structure achieves broadband radiation, with low RCS and high gain, in the propagation direction whereas broadband absorption is achieved, when it is exposed to a free space plane wave. Moreover, the metamaterial absorber has stable absorptivity for an incident angle of (0°–30°). To verify the in-band absorption and radiation of the proposed design, a 6×6 periodic array of resonators has been fabricated and experimentally verified in an anechoic chamber. The measured results validate the performed simulations.

INDEX TERMS Metasurface-absorber, metasurface antenna, low RCS.

I. INTRODUCTION

Metamaterial absorbers have attracted much interest for many years for their unique properties; they can be integrated with several devices to improve the desired performance such as radar cross section (RCS). The RCS reduction implies the decreasing of the observability of a radiating structure and it has an application in stealth technology. The observability of an antenna can be reduced by means of shaping [1], using absorbing materials [2], using passive or active elements such as diodes [3] and by using metamaterial structures [4]. For example, in [1] the RCS of a monopole antenna is reduced by applying the principle of bionics. The low RCS antenna is designed by using a model of insect tentacle. The artificially designed resonating structures mainly have significant impact in low observable antennas [4]–[7]. Artificially designed resonating structures present a specific configuration such as circular shaped [5], square shaped [6] and triangular shaped [7] geometries. For example, a Tri-band metamaterial absorber has been designed for X band application using circular shaped metallic rings that operate at tri-narrow bands [5]. Alternatively, a wearable microwave absorber has been designed with more than 90% absorption for narrow band applications [6]. Similarly, compact circular ring resonator exhibits more than 90% absorption at narrow band, *i.e.* from 1.3–3.5 GHz [8]. In the literature, the designed metamaterial absorbers are used to reduce the RCS of narrow band antennas. In addition, in the previous research work, the metamaterial structure contributes in absorption but it does not contribute in terms of electromagnetic radiation. However, they are designed separately and combined with an antenna for the RCS reduction [9]–[17]. For example, an active reconfigurable frequency selective surface (FSS) has been designed to reduce the RCS of a patch antenna [12]. The designed reconfigurable FSS reflector is able to switch the stop-band to a pass-band using a diode. Left handed materials have been designed to reduce the RCS of microstrip patch antenna [9]. Similarly, in [10] the RCS reduction of a microstrip antenna is based upon electromagnetic bandgap (EBG) absorber using a conducting polymer.

The associate editor coordinating the review of this manuscript and approving it for publication was Qammer Hussain Abbasi.

Also in [14], [15] holographic metasurfaces are designed to reduce the RCS of the regular patch antenna. To design metasurface structures with the alternating function of wideband absorption and radiation is a challenging task. Nevertheless, considerable effort has been made to integrate a narrowband absorber with an antenna [10], [16]–[18]. The reported structures are a combination of metamaterial absorbers and antenna, but limited to a single frequency operation. This may cause malfunction in some high data rate communications systems [19]–[26].

Another issue related to the reported structures is a tradeoff between RCS and gain. In fact, the RCS reduction may cause degradation in gain. For example, in [12] and [13] when an FSS reflector is applied to an antenna, it degrades the gain by 0.3 dB and 1.5 dB, respectively. Similarly, when a metamaterial absorber is added to an antenna, the gain of the antenna is reduced by 0.53 dB [17]. Moreover, the reported implementations are unable to provide wideband absorption and radiation, alternatively.

In this paper, we present a periodic structure, which can alternate between electromagnetic radiation and absorption. The proposed multilayered structure consists of two F4B substrates with a dielectric constant of $\varepsilon_r = 2.65$. The metamaterial structure has a low RCS about -10 dB within the operating band from 7.5 GHz to 9.5 GHz and wideband gain of 9-11 dB.

This paper is organized as follows. In Section II, the working principle of the dual function metasurface model for both radiation and absorption is explained. In Section III, the metamaterial absorber design and the simulated and measured results are discussed. In Section IV, the feeding network and its implantation to achieve the functionality of a metasurface antenna are presented. Finally, the main conclusions are drawn in Section V.

II. DUAL-FUNCTIONAL MODEL CONCEPT

The dual-function concept is demonstrated by using single-pole double-throw switches (SPDTs). The working principle of both absorber and radiator is depicted in FIGURE 1 using SPDTs switches. The proposed model has two states, *i.e.*, state "A" for the radiating mode and state "B" for the absorber mode.

In state "A", the switch 'S_1' is connected to a load, whose impedance is R_r (playing the role of the radiation resistance) and the switch S_2 is connected to the input source signal. Therefore, in state "A", the proposed dual function structure corresponds to the equivalent circuit of an antenna. According to the theory of antennas [27], the input impedance of a radiating antenna is;

$$Z_{in(antenna)} = R_r + R_L + jX \tag{1}$$

where, R_r is the radiation resistance causing the radiation into space, R_L is the loss resistance and X represents the reactance of the antenna.

To achieve a metamaterial absorbing function, in state "B", S_1 is connected to an equivalent plane wave source

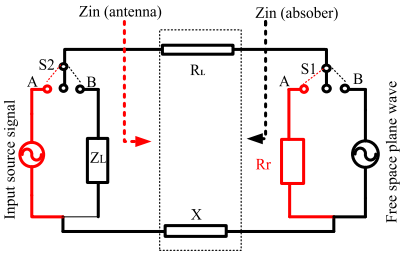

FIGURE 1. Equivalent circuit model of the multifunctional metasurface acting as a radiator and absorber.

and S_2 is connected to a load whose impedance value is Z_L. Under this condition, the incident plane wave represents the excitation of the absorber as shown in FIGURE 1. The input impedance of the absorber can be defined as;

$$Z_{in(absorber)} = Z_L + R_L + jX \tag{2}$$

where Z_L represents a lumped resistance, R_L and X_L denote the impedance of the absorber. From the aforementioned equivalent circuit model, it is clear that the metamaterial absorbing structure can also be used as a metasurface antenna.

III. METAMATERIAL ABSORBER SIMULATIONS AND MEASUREMENTS RESUTLS

A. DESIGN OF METAMATERIAL UNIT CELL

The schematic diagram of the designed metamaterial unit cell is shown in FIGURE 2. The proposed metasurface is a periodic array of sub-wavelength resonant scatters, which control the electromagnetic response of the surface [28], [29], and consists of distinct metallic elements (a square ring resonator and PEC ground) on each side of the upper substrate. The upper substrate is fully grounded and thus, it presents a very low transmission level. The equivalent circuit of the proposed metamaterial unit cell is shown in FIGURE 2(c).

For an electromagnetic normally incident wave, the symmetric square metal ring acts as an electric inductive-capacitive (LC) resonator, supplying the electric coupling to the incident electric field. The antiparallel currents between the metallic square loop and ground metal film create the magnetic coupling to the incident magnetic field. The suggested square loop structure was studied in [30] as a FSS based metamaterial absorber that provides a narrow band absorption. However, to enhance the absorption level, three lumped resistors ($R = 140\ \Omega$) are inserted into the unit cell. The periodic array of single square loops are etched on the metallic substrate. As shown in The equivalent circuit of the proposed metamaterial unit cell is shown in FIGURE 2(c), the circuit model of the proposed unit cell is composed of an RLC series circuit, where C and L are the total equivalent capacitance and inductance, respectively. The free space impedance $Z_0 = 377\ \Omega$ and the dielectric slab impedance is $Z_{01} = Z_0/\sqrt{\varepsilon r} = 231.6\ \Omega$. Based on the overall equivalent circuit model, we can determine that the equivalent circuit of a metamaterial unit cell corresponds to an LC resonant tank. The square loop resonator is described by the means

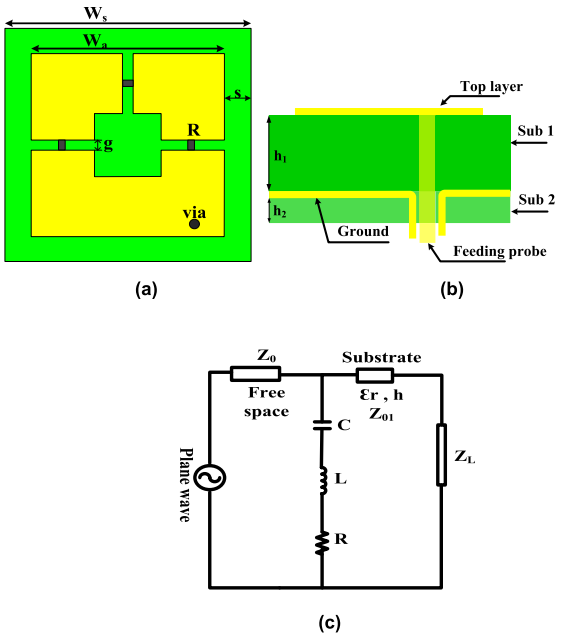

FIGURE 2. (a) Geometrical model of the proposed metamaterial unit cell, with dimension of $W_s = 19.5$ mm $W_a = 13.5$ mm, $s = 3$ mm and $g = 0.8$ mm $h_1 = 3$, $h_2 = 1$, (b) side view and its (c) equivalent circuit model.

of the parameters W_s, W_a, s and g. The resonant frequency is directly proportional to $1/\sqrt{}$ LC where, L and C are the equivalent capacitance and inductance respectively, as shown in FIGURE 2(c).

B. SIMULATED AND MEASURED RESULTS

Numerical simulations were carried out using Microwave Studio CST 2016 based on the finite integration method. The condition of perfect electric field in x-direction and perfect magnetic in y-direction boundaries are applied to the transverse to account for the plane electromagnetic wave, with the wave propagating along the z-direction (k-direction) are set to be open boundaries. The optimized dimensions of the resonating metamaterial unit cell is $0.5\lambda \times 0.5\lambda$ and the spacing among two unit cell is $0.16\lambda \times 0.16\lambda$, whereas the free space wavelength 'λ' is considered at center frequency of 8 GHz. Since the backside of the upper substrate is fully metallic, as shown in FIGURE 2(b), the transmission coefficient is expected to be approximately zero. However, due to the feed network and vias, the transmission coefficient has to be carefully considered. Based on a tuning optimization simulation process, a final prototype of 6×6 unit cells has been designed, fabricated and tested.

The simulated and measured electromagnetic resonance behaviors of the proposed structure are shown in FIGURE 3(a) - (c). FIGURE 3(a) depicts the simulated and measured reflection coefficient. It is observed that reflectivity is lower than -10 dB from 7.5 GHz to 9.5 GHz.

The wideband absorption, A(w), can be calculated by using $A(w) = 1 - T(w) - R(w)$, where $T(w) = |S_{12}|^2$ and $R(w) = |S_{11}|^2$ are the transmission and reflectance

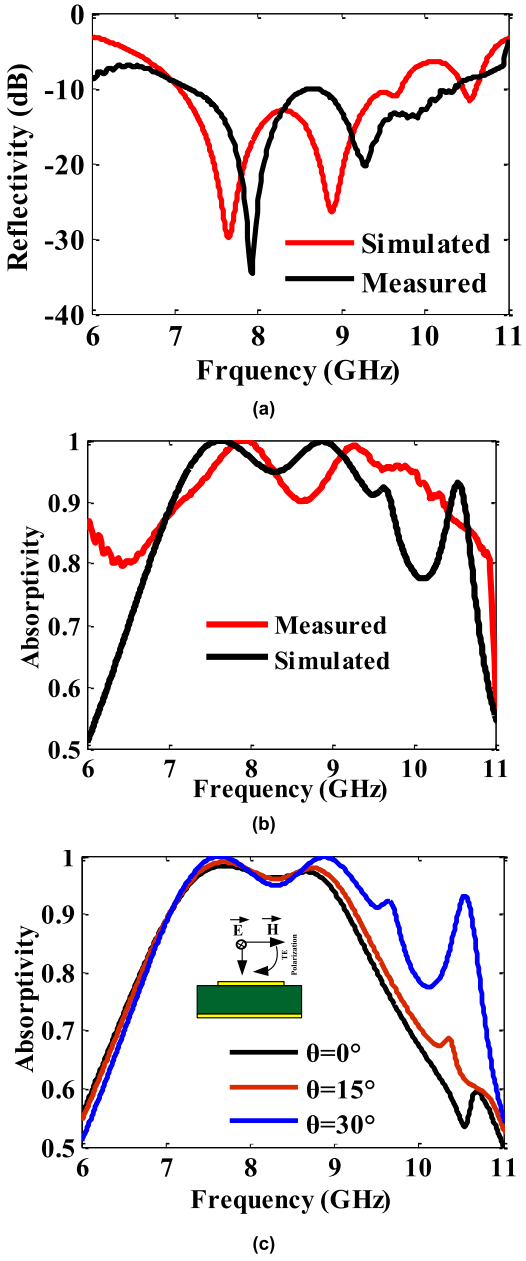

FIGURE 3. (a) Reflectivity (b) absorption characteristics of metasurface and (c) absorption effect of the incident angle.

coefficients, respectively [31]. The transmission coefficient, $T(w)$, is very low, but cannot be ignored. For a normal incident electromagnetic wave, the simulated and measured absorption characteristics are depicted in FIGURE 3(b).

It is clear from the FIGURE 3(b), that the absorptivity is more than 90% over the resonant frequency range of 7.5–10 GHz. The total dimension of the fabricated metasurface is about $2.96\lambda \times 2.96\lambda$ at 8 GHz therefore, measurements were performed carefully, but still there is a discrepancy between measured and simulated results, which can be attributed to the fabrication tolerances and the measuring environmental influence.

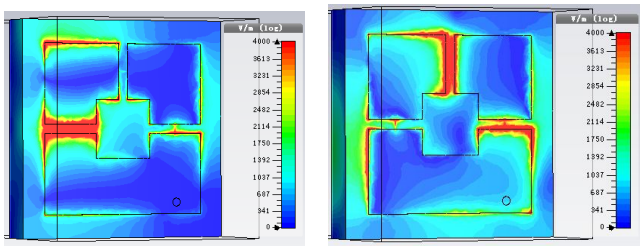

(a) (b)

FIGURE 4. Electric field distribution for wideband metamaterial absorber at (a) 8 GHz and (b) 9 GHz.

FIGURE 3(c) shows the simulated absorptivity as a function of frequency at various incident angles for TE polarization. For incident angle from 0° to 30° the absorptivity is greater than 0.9 or 90% in the operating band, which means that the metamaterial resonator absorptivity performance remains high and stable.

To demonstrate the physical behavior of the metamaterial absorber, the E-field distribution has been simulated at resonance frequencies. FIGURE 4(a) & (b), show the simulated E-field distribution of the metamaterial unit cell at 8 GHz and 9 GHz. It can be seen that the E-field distribution is strong between PEC and metallic resonator showing a strong dielectric loss that causes the absorption.

In order to integrate the antenna and absorber, a multilayered PCB is designed having two dielectric substrates. The architecture of the proposed integrated structure is shown in FIGURE 5 (a)–(d). The metallic loops are symmetrically placed on an F4B substrate with dielectric constant of 2.65 and thickness of a 3 mm and each metallic loop is fed through vias from the bottom layer as shown in FIGURE 2(b) side view.

IV. DESIGN OF METASURFACE RADIATOR

In this section, the same designed metasurface structure (explained in section III) is demonstrated as a metamaterial radiator or antenna, where the working principle of the proposed multifunctional equivalent circuit model is explained in section II. To excite each resonator, a feeding network is designed on the backside of metasurface. For the feeding network, an additional F4B substrate having a thickness of 1 mm has been added to the multilayered implementation. The feeding network is designed in a way that it connects all resonators to a single 50 Ω feed line as shown in FIGURE 5(b).

A via with a diameter of 0.6 mm according to the fabrication constraint is chosen to connect the feed line with the square loop patch. The position of the via is heuristically optimized to get optimum matching. The matching circuit is based on microstrip feed lines. All radiators are fed in order to achieve the highest gain in z-direction.

A. DESIGN OF 3×3 AND 6×6 ANTENNA ARRAY

Simulations have been carried out to analyze the performance of 3×3 and 6×6 antenna elements. The architecture of the proposed 3×3 multilayered design and its feeding network is shown in FIGURE 5(a) and (b) whereas the architecture of the final designed structure is shown in FIGURE 5 (c) and (d).

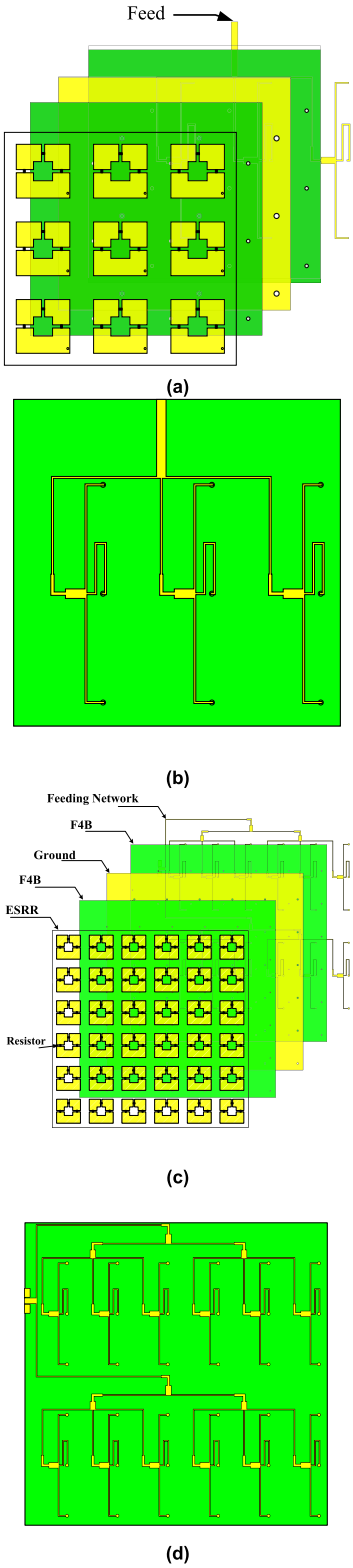

FIGURE 5. Architecture of the proposed structure for (a) multilayered 3×3 antenna array and its (b) feeding network, (c) multilayered 6×6 antenna array and its (d) feeding network.

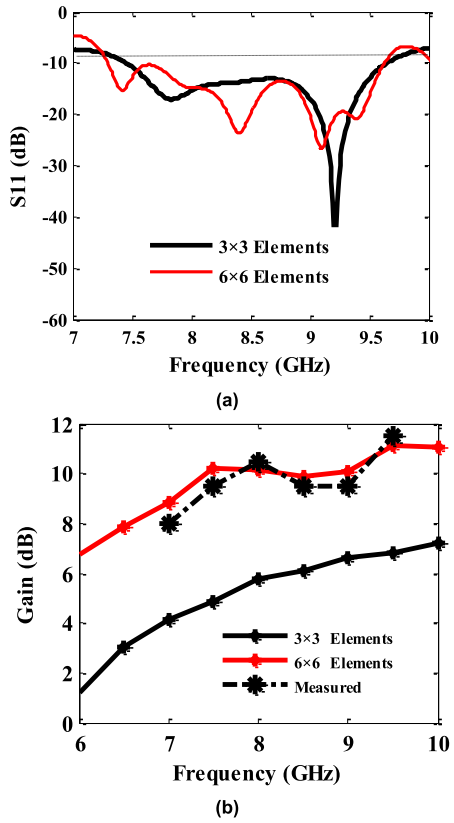

FIGURE 6. Simulated (a) return loss and (b) peak gain of the of 3×3 and simulated and measured gain of the 6×6 antenna arrays.

The simulated return loss for the 3×3 and 6×6 antenna elements is shown in FIGURE 6 (a). As can be seen from FIGURE 6 (a), both 3×3 and 6×6 unit elements have almost the same impedance matching from 7.5 GHz to 9.5 GHz. The simulated peak gain of 3×3 and 6×6 unit elements is depicted in FIGURE 6(b). The peak gain for 3×3 unit elements is varying around 4.2 dB whereas the peak gain is increased for 6×6 unit elements to around 11 dB in the resonating band as shown in FIGURE 6(b). The maximum gain 11.2 dB is achieved at resonance frequency of 9.5 GHz.

B. SIMULATED AND MEASURED RESULTS

To realize the proposed metasurface antenna, a planar array of 6×6 unit elements is manufactured on multilayered F4B substrates. The fabricated multilayered prototype is depicted in FIGURE 7(a) and (b). The experiments are carried out with an N5245A network analyzer in an anechoic chamber. The measured results of the 6×6 antenna array are shown in FIGURE 8(a)–(c).

FIGURE 8(a) shows that the measured return loss is less than −10 dB from 7.5 GHz to 9.5 GHz. The simulated and measured return losses are in good agreement. In FIGURE 8(b), the radiation and total efficiencies of the designed metasurface antenna are plotted at resonance frequencies: 7.5, 8, 8.5, 9 and 9.5 GHz. The maximum radiation efficiency of 83.9% is observed at 8 GHz.

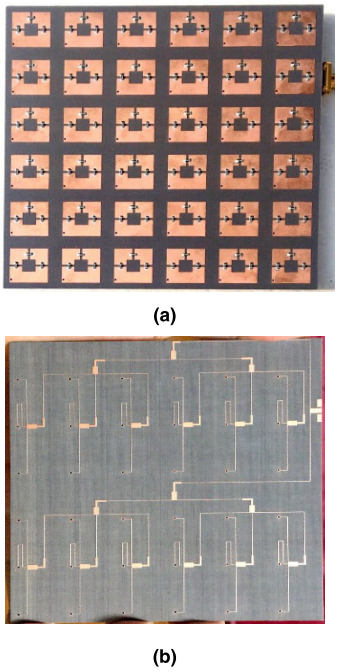

FIGURE 7. Fabricated prototype of the proposed design (a) top view and (b) bottom view.

TABLE 1. Comparison of the proposed metasurface with previously designed regular patch antennas.

Ref.	Bandwidth	Alternate function		Efficiency	Gain (dB)
		Radiation	Absorption		
This work	Broadband	Yes	Yes	>65%	9.5–11.2
[11]	Narrowband	Yes	No	75%	6.65
[10]	Narrowband	Yes	No	85%	6
[17]	Narrowband	Yes	No	Not given	NA
[15]	Wideband	Yes	No	Not given	12
[14]	Narrowband	Yes	No	Not given	10

In order to verify the RCS reduction performance of the designed metasurface structure, the time domain solver in CST is used, considering all the boundary conditions set to be open. The monostatic RCS of the proposed metasurface antenna and its comparison with a PEC (equal size of antenna ground) is depicted in FIGURE 8(c). In FIGURE 8(c), the RCS curve versus frequency is plotted for a normal incident plane wave. FIGURE 8(c) shows an obvious reduction in RCS in the whole operation band (7.5 – 9.5 GHz) of the designed metasurface antenna.

To further investigate the principle of RCS reduction, the bistatic RCS comparison with the PEC and the proposed metasurface antenna is shown in FIGURE 9(a) & (b) at 8 GHz and 9 GHz when $\phi = 0°$ (E-plane). The RCS is significantly reduced in the angular region $-80° \leq \theta \leq 80°$, where the largest reduction is observed at 0°. However, little increment is observed in the angular region such as $-80° \leq \theta \leq -150°$ and $80° \leq \theta \leq 150°$. This fact may be due to the anomalous scattering energy. The E-field and H-field radiation pattern are also depicted in FIGURE 10(a) and (b). It can be observed

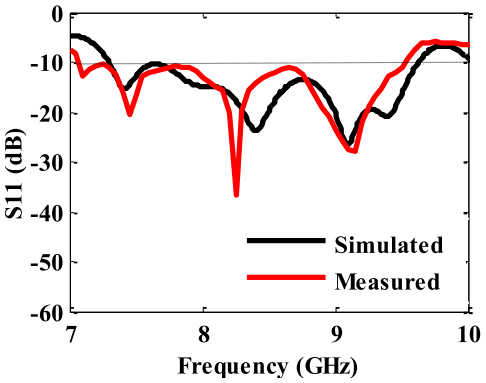

(a)

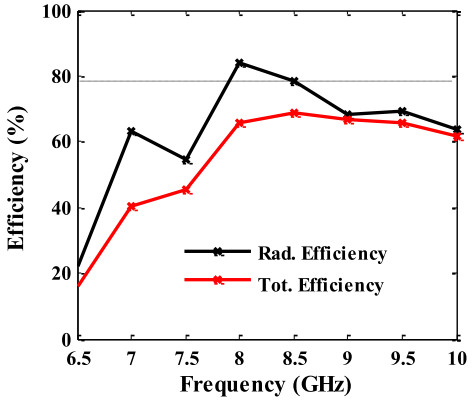

(b)

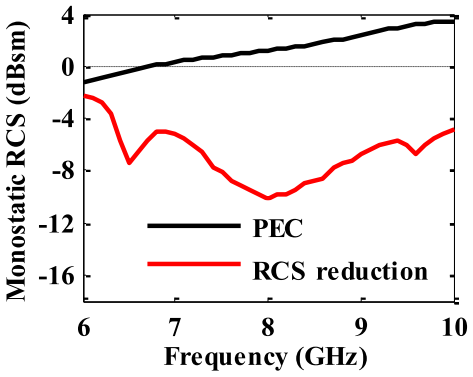

(c)

FIGURE 8. (a) Simulated and measured return loss (b) total efficiency and radiation efficiency and (c) monostatic RCS of the proposed metasurface antenna.

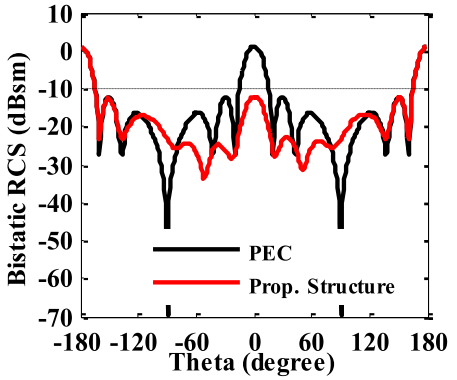

(a)

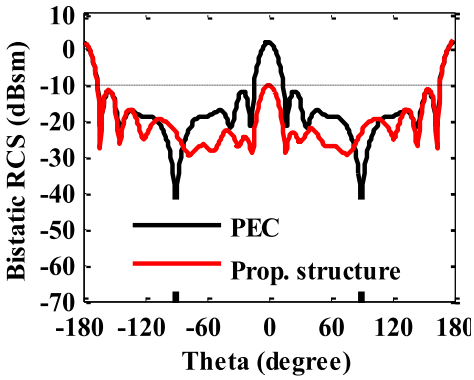

(b)

FIGURE 9. Bistatic RCS of the metasurface antenna when $\phi = 0°$ at (a) 8 GHz (b) 9 GHz.

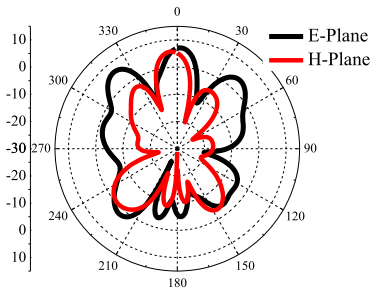

(a)

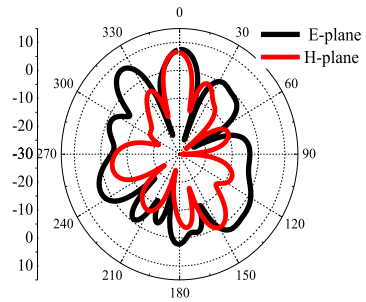

(b)

FIGURE 10. E-Plane and H-Plane radiation patterns at (b) 8 GHz and (c) 9 GHz.

that the main lobe is generally directed towards the normal direction at 8 GHz and 9 GHz.

The performance of the proposed metasurface structure, and previously designed metamaterial based on patch antennas from the state of the art are listed in Table 1. It can be concluded that the previously designed metamaterial based on patch antennas present low RCS but they have no alternate in-band absorption and radiation feature. In addition, the previously designed metamaterial loaded patch antennas have a trade-off in terms of RCS and gain, since the reduction in RCS implies that the gain of the patch antenna decreases. Therefore, it is highlighted that the proposed metamaterial antenna is able to satisfy both requirement of high gain and low RCS performance. Moreover, the previously designed antennas provide a narrowband frequency range, whereas the proposed metasurface antenna presents wideband operation.

V. CONCLUSION

A dual-function metasurface structure has been designed with alternating absorption and radiation characteristics. Simulated and experimental results validate the designed metamaterial structure. The proposed design is implemented on a multilayered PCB providing a wideband absorption and high gain radiation. To validate the design, two 3×3 and 6×6 antenna elements are simulated and the 6×6 unit element array has been fabricated. The proposed design is experimentally verified showing a gain of 11dB from 7.5 GHz to 9.5 GHz and -10 dB reduction in RCS. The proposed metasurface antenna provides an alternative way to design planar antenna array with high gain, low RCS and beam steering capability.

REFERENCES

[1] W. Jiang, Y. Liu, S. Gong, and T. Hong, "Application of bionics in antenna radar cross," *IEEE Antennas Wireless Propag. Lett.*, vol. 8, pp. 1275–1278, 2009.

[2] F. Wang, W. Jiang, S. Gong, Y. Zhang, T. Hong, and H. Xue, "Radar cross section reduction of wideband antenna with a novel wideband radar absorbing materials," *IET Microw., Antennas Propag.*, vol. 8, no. 7, pp. 491–497, May 2014.

[3] Y. Shang, S. Xiao, M.-C. Tang, Y.-Y. Bai, and B. Wang, "Radar cross-section reduction for a microstrip patch antenna using PIN diodes," *IET Microw. Antennas Propag.*, vol. 6, no. 6, p. 670, 2012.

[4] Y. Cheng and H. Yang, "Design, simulation, and measurement of metamaterial absorber," *J. Appl. Phys.*, vol. 108, no. 3, Aug. 2010, Art. no. 034906.

[5] O. B. Ayop, M. K. A. Rahim, N. A. Murad, N. A. Samsuri, and R. Dewan, "Triple band circular ring-shaped metamaterial absorber for X-band applications," *Prog. Electromagn. Res. M*, vol. 39, pp. 65–75, 2014.

[6] J. Tak and J. Choi, "A wearable metamaterial microwave absorber," *IEEE Antennas Wireless Propag. Lett.*, vol. 16, pp. 784–787, 2017.

[7] H. F. Zhang, H. Zhang, Y. Yao, J. Yang, and J.-X. Liu, "A band enhanced plasma metamaterial absorber based on triangular ring-shaped band enhanced plasma metamaterial absorber absorber based on triangular," *IEEE Photon. J.*, vol. 10, no. 4, pp. 1–11, Aug. 2018.

[8] M. D. Banadaki, A. A. Heidari, and M. Nakhkash, "A metamaterial absorber with a new compact unit cell," *IEEE Antennas Wireless Propag. Lett.*, vol. 17, no. 2, pp. 205–208, Feb. 2018.

[9] J. K. Zhang, J. C. Xu, J. Ding, and C. J. Guo, "Low radar cross section microstrip antenna based on left-handed material," *Microw. Opt. Technol. Lett.*, vol. 61, no. 6, pp. 1559–1565, Jun. 2019.

[10] H.-K. Jang, W.-J. Lee, and C.-G. Kim, "Design and fabrication of a microstrip patch antenna with a low radar cross section in the X-band," *Smart Mater. Struct.*, vol. 20, no. 1, Jan. 2011, Art. no. 015007.

[11] Y. Liu and X. Zhao, "Perfect absorber metamaterial for designing low-RCS patch antenna," *IEEE Antennas Wireless Propag. Lett.*, vol. 13, pp. 1473–1476, 2014.

[12] F. Wang, K. Li, Y. Ren, and Y. Zhang, "A novel reconfigurable FSS applied to the antenna radar cross section reduction," *Int. J. RF Microw. Comput. Aided Eng.*, vol. 29, no. 7, Jul. 2019, Art. no. e21729.

[13] M. Z. Joozdani, M. K. Amirhosseini, and A. Abdolali, "Wideband RCS reduction of patch array antenna with miniaturized FSS," *Microw. Opt. Technol. Lett.*, vol. 58, no. 4, pp. 969–973, Apr. 2016.

[14] Y. Liu, N. Li, Y. Jia, W. Zhang, and Z. Zhou, "Low RCS and high-gain patch antenna based on a holographic metasurface," *IEEE Antennas Wireless Propag. Lett.*, vol. 18, no. 3, pp. 492–496, Mar. 2019.

[15] M. Long, W. Jiang, and S. Gong, "RCS reduction and gain enhancement based on holographic metasurface and PRS," *IET Microw., Antennas Propag.*, vol. 12, no. 6, pp. 931–936, May 2018.

[16] Z.-X. Zhang and J.-C. Zhang, "RCS reduction for patch antenna based on metamaterial absorber," in *Proc. Progr. Electromagn. Res. Symp. (PIERS)*, vol. 4, Aug. 2016, pp. 8–11.

[17] T. Liu, X. Cao, J. Gao, Q. Zheng, W. Li, and H. Yang, "RCS reduction of waveguide slot antenna with metamaterial absorber," *IEEE Trans. Antennas Propag.*, vol. 61, no. 3, pp. 1479–1484, Mar. 2013.

[18] Y.-Q. Li, H. Zhang, Y.-Q. Fu, and N.-C. Yuan, "RCS reduction of ridged waveguide slot antenna array using EBG radar absorbing material," *IEEE Antennas Wireless Propag. Lett.*, vol. 7, pp. 473–476, 2008.

[19] S. A. Shah, D. Fan, A. Ren, N. Zhao, X. Yang, and S. A. T. Tanoli, "Seizure episodes detection via smart medical sensing system," *J. Ambient Intell. Humaniz. Comput.*, pp. 1–13, Nov. 2018, doi: 10.1007/s12652-018-1142-3.

[20] X. Yang, D. Fan, A. Ren, N. Zhao, S. Aziz, and S. Akram, "Diagnosis of the hypopnea syndrome in the early stage," *Neural Comput. Appl.*, vol. 8, no. 1, pp. 1–12, 2019.

[21] D. Haider, A. Ren, D. Fan, N. Zhao, X. Yang, S. A. Shah, F. Hu, and Q. H. Abbasi, "An efficient monitoring of eclamptic seizures in wireless sensors networks," *Comput. Electr. Eng.*, vol. 75, pp. 16–30, May 2019.

[22] Q. Zhang, D. Haider, W. Wang, S. Shah, X. Yang, and Q. Abbasi, "Chronic obstructive pulmonary disease warning in the approximate ward environment," *Appl. Sci.*, vol. 8, no. 10, p. 1915, Oct. 2018.

[23] S. Tanoli, M. Rehman, M. Khan, I. Jadoon, F. Ali Khan, F. Nawaz, S. Shah, X. Yang, and A. Nasir, "An experimental channel capacity analysis of cooperative networks using universal software radio peripheral (USRP)," *Sustainability*, vol. 10, no. 6, p. 1983, Jun. 2018.

[24] M. B. Khan, X. Yang, A. Ren, M. A. M. Al-Hababi, N. Zhao, L. Guan, D. Fan, and S. A. Shah, "Design of software defined radios based platform for activity recognition," *IEEE Access*, vol. 7, pp. 31083–31088, 2019.

[25] S. A. Shah and F. Fioranelli, "RF sensing technologies for assisted daily living in healthcare: A comprehensive review," *IEEE Aerosp. Electron. Syst. Mag.*, vol. 34, no. 11, pp. 26–44, Nov. 2019.

[26] D. Haider, A. Ren, D. Fan, N. Zhao, X. Yang, S. A. K. Tanoli, Z. Zhang, F. Hu, S. A. Shah, and Q. H. Abbasi, "Utilizing a 5G spectrum for health care to detect the tremors and breathing activity for multiple sclerosis," *Trans. Emerg. Telecommun. Tech*, vol. 29, no. 10, Oct. 2018, Art. no. e3454.

[27] C. A. Balanis, *Antenna Theory: Analysis and Design*, 3rd ed. Hoboken, NJ, USA: Wiley, 2008.

[28] N. Yu and F. Capasso, "Flat optics with designer metasurfaces," *Nature Mater.*, vol. 13, no. 2, pp. 139–150, Feb. 2014.

[29] S. S. Bukhari, J. Vardaxoglou, and W. Whittow, "A metasurfaces review: Definitions and applications," *Appl. Sci.*, vol. 9, no. 13, p. 2727, Jul. 2019.

[30] S. Ghosh and K. V. Srivastava, "An equivalent circuit model of FSS-based metamaterial absorber using coupled line theory," *IEEE Antennas Wireless Propag. Lett.*, vol. 14, pp. 511–514, 2015.

[31] N. I. Landy, S. Sajuyigbe, J. J. Mock, D. R. Smith, and W. J. Padilla, "Perfect metamaterial absorber," *Phys. Rev. Lett.*, vol. 100, no. 20, 2008, Art. no. 207402.

SAEED UR RAHMAN was born in 1989. He received the B.S. degree in electronics engineering from COMSAT University, Pakistan, in 2013, and the M.S. degree in electronics engineering from the Capital University of Science and Technology (CUST), Pakistan, in 2016. He is currently pursuing the Ph.D. degree with the Nanjing University of Aeronautics and Astronautics (NUAA), Nanjing, China. His research interests include electromagnetics and antennas especially designing, and optimization of antenna array, micro-strip patch antennas, ultra wideband antennas and meta-materials absorbers, FSS, and polarization conversation.

QUNSHENG CAO received the Ph.D. degree in electrical engineering from The Hong Kong Polytechnic University, Hong Kong, in 2000. From 2000 to 2005, he worked as a Research Associate with the Department of Electrical Engineering, University of Illinois at Urbana–Champaign and the Army High-Performance Computing Research Center, University of Minnesota, USA. In 2006, he joined the Nanjing University of Aeronautics and Astronautics, China, as a Professor of electrical engineering. He has authored more than 190 academic articles in refereed international journals and conference proceedings. His current research interests include computational electromagnetics, microwave, and antennas technologies and radar signal processing. His research team is also engaged in high-speed circuit signal integrity, antenna, microwave components, and new method in radar signal processing.

IGNACIO GIL was born in Barcelona, Spain, in 1978. He received the degrees in physics and electronics engineering, in 2000 and 2003, respectively, and the Ph.D. degree from the Universitat Autònoma de Barcelona, Spain, in 2007. From 2003 to 2008, he was an Assistant Professor of electronics and a Researcher with the RF-Microwave Group, Electronic Engineering Department, Universitat Autonòma de Barcelona. From 2006 to 2008, he worked for EPSON Europe Electronics GmbH, where he developed high-performance integrated RF CMOS circuits, transceivers, and system design. In 2008, he joined the Electronic Engineering Department, Universitat Politècnica de Catalunya (UPC), Spain, as a Lecturer and a Researcher, where he has been an Associate Professor, since 2011. Since 2012, he has been a Collaborator with the Universitat Oberta de Catalunya (UOC), Spain. From 2012 to 2014, he served as the Chairman of the Spanish IEEE EMC Chapter. In 2017, he was an Academic Visitor with the Wireless Communications Research Group, Loughborough University (U.K.). His research activities and interests include passive and active RF and microwave devices and circuits, metamaterials, EMC, and smart textile electronics.

MUHAMMAD SAJJAD was born in 1990. He received the B.S. degree in telecommunication from the University of Science and Technology, Bannu, Pakistan, in 2013, and the M.S. degree in electrical engineering from COMSAT University, Pakistan, in 2017. He is currently pursuing the Ph.D. degree with the Nanjing University of Aeronautics and Astronautics (NUAA), Nanjing, China. His research interests include electromagnetics and antennas especially metasurfaces, FSS, and polarization conversation.

YI WANG (Member, IEEE) received the B.S. and Ph.D. degrees in communication and information system from the Nanjing University of Aeronautics and Astronautics (NUAA), Nanjing, China, in 2006 and 2012, respectively. In 2012, he joined the College of Electronic and Information Engineering, NUAA, as an Assistant Professor, where he is currently working as an Associate Professor. His research interests include computational electromagnetics, especially the finite difference time-domain (FDTD) method, the FDTD modeling of the entire earth-ionosphere systems, and the earthquake electromagnetics, and research focuses on the FDTD simulation of anisotropic media, and earthquake phenomena.